

Temperature dependence of NMR Knight shift in pnictides: proximity to a van Hove singularity

R. Nourafkan, S. Acheche

*Institut quantique & Département de Physique and RQMP,
Université de Sherbrooke, Sherbrooke, Québec, Canada J1K 2R1*

(Dated: July 26, 2018)

The unconventional temperature variation of the Knight shift (static spin susceptibility) that has been observed in Fe-based superconductors AFe_2As_2 ($A = \text{K, Rb, Cs}$) is explained in terms of proximity to a van Hove singularity. Using the Hubbard model we show that when the Fermi energy is in the vicinity of a van Hove singularity, a downturn in spin susceptibility occurs as the temperature is lowered. This behavior is characterized by a temperature, T^* , which is determined by the difference in energy between the Fermi level and the van Hove singularity. When vertex corrections are taken into account in a dynamical mean-field approximation, the effect of correlations amplifies the relative drop in the Knight shift and moves T^* to lower temperatures.

PACS numbers: 74.70.Xa, 71.27.+a

Nuclear magnetic resonance (NMR) techniques provide a probe of the spin response at specific atomic locations. In an itinerant electron system, the spin part of the Knight shift measured in NMR experiments is proportional to the uniform spin susceptibility, $K_S(T) = B\chi^m(T)$ where B denotes the hyperfine coupling describing coupling between nuclear spins and itinerant electron spins. The hyperfine coupling is temperature independent, hence, the temperature dependence of the Knight shift, K_S , is identical with that of spin susceptibility. The spin susceptibility of itinerant electrons is given by the Pauli susceptibility. For non-interacting systems, χ^m takes the form $(1/4) \int d\epsilon \rho(\epsilon) (dn(\epsilon)/d\epsilon)$ where $n(\epsilon)$ is the Fermi distribution function and $\rho(\epsilon)$ denotes the total density of states. It depends weakly on the temperature and upon decreasing temperature smoothly saturates to its $T = 0$ limit, i.e., $\sim \rho(\epsilon_F)/4$, where ϵ_F is the Fermi energy.

In heavy Fermion systems with both localized f electrons and itinerant conduction electrons c , the temperature dependence of the Knight shift may differ from the temperature dependence of the total spin magnetization. This so-called Knight shift anomaly can be understood in terms of two hyperfine couplings to the two different electron spins (localized vs itinerant)¹. Then the Knight shift is given by $K_S = B_1\chi_{cc}^m + (B_1 + B_2)\chi_{cf}^m + B_2\chi_{ff}^m$, i.e. Knight shift weighs the different correlation functions separately. At temperatures higher than a material-dependent characteristic temperature, $T > T^X$, the Curie-Weiss susceptibility of the local moments dominates the temperature-independent Pauli susceptibility of the conduction electrons, then $K_S \simeq B_2\chi_{ff}^m$. Therefore, K_S monotonically increases upon decreasing T for these values of temperature. Below T^X , χ_{cf}^m becomes significant and governs the temperature dependence of the Knight shift, which is different from the Curie-Weiss law¹.

Recently, a similar Knight shift anomaly (crossover) was observed in heavily hole-doped Fe-based superconductors AFe_2As_2 ($A = \text{K, Rb, Cs}$); at low temperature the Knight shift deviates from a Curie-Weiss behavior describing the high temperature regime^{2,3}. A similar behavior is seen for the spin susceptibility of KFe_2As_2 ³. The characteristic crossover temperature, T^* , decreases continuously when K is substituted with the larger alkaline ions Rb or Cs. Below T^* , the Knight shift decreases upon decreasing T and eventually saturates at

very low temperature. Due to the similarity and observed large effective masses in these compounds, it was suggested that the Knight shift crossover in AFe_2As_2 can indicate an orbital-selective Mott transition in which electrons in the d_{xy} orbital undergo a Mott transition and become localized while electrons in d_{xz} and d_{yz} remain itinerant²⁻⁵. However, this scenario is highly debated for iron-based superconductors which are believed to be Hund's metal with the multiorbital nature as the key factor⁶⁻⁸.

Here we propose an alternative explanation of this behavior. Indeed, a van Hove singularity (vHS) has been observed in angle-resolved photoemission spectroscopy (ARPES) of AFe_2As_2 and confirmed by LDA calculation⁹. The vHS is located just a few meV below the Fermi level and moves towards it upon substitution of K with Rb or Cs. The proximity of the vHS can induce a pronounced temperature dependence of the Pauli susceptibility. It has also been proposed as responsible for both the heavy mass behavior observed in these materials, and for their superconducting gap symmetry^{9,10}. Here, we show that the Knight shift shows a similar crossover due to the proximity of the vHS. We show that the characteristic temperature T^* scales with the difference in energy between the Fermi level and the position in energy of the vHS, ϵ_{vHS} ; it moves to higher temperature upon increasing this energy difference. Furthermore, $K_S(T^*) - K_S(T \rightarrow 0)$ decreases when the Fermi level is located further away from ϵ_{vHS} . We also investigate the effect of electron-electron interactions on this behavior. We find that upon increasing electron-electron interaction, $K_S(T^*) - K_S(T \rightarrow 0)$ increases and T^* shifts to lower temperatures.

Model and method – The influence of a vHS on the Knight shift can be discussed using the Hubbard model on the square lattice,

$$H = -t \sum_{\langle ij \rangle \sigma} c_{i\sigma}^\dagger c_{j\sigma} + U \sum_i n_{i\uparrow} n_{i\downarrow}, \quad (1)$$

where $c_{i\sigma}^\dagger (c_{i\sigma})$ creates (annihilates) an electron with spin σ on site i and $n_{i\sigma} = c_{i\sigma}^\dagger c_{i\sigma}$. The amplitude t denotes the nearest-neighbor hopping amplitude, and U the on-site screened Coulomb interaction. The non-interacting density of states of this model possesses a vHS at zero energy. At

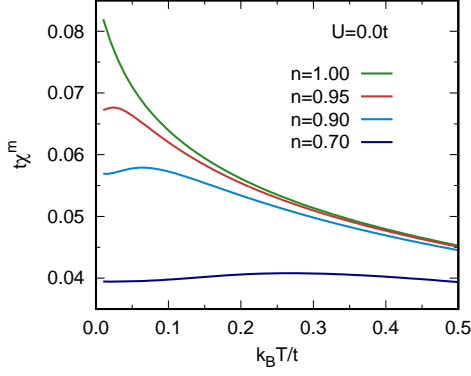


FIG. 1. Knight shift $K_S \propto \chi^m$ of the non-interacting system as a function of temperature $k_B T/t$ for several electron densities. The peak position of the Knight shift moves to higher temperature and become less pronounced when Fermi energy moves away from vHS location.

half-filling the Fermi energy lies on the ϵ_{vHS} . This model also allows us to discuss the impact of correlations on the temperature dependence of the Knight shift. The model has particle-hole symmetry, hence similar results would be obtained whether the vHS is located above or below Fermi level.

In general, the Pauli susceptibility is determined by the $\mathbf{q} \rightarrow 0$ and $\nu_n \rightarrow 0$ limit of $\chi_{ph}^m(\mathbf{q}, \nu_n)$ where χ_{ph}^m is the lattice magnetic susceptibility. In an interacting system, the so-called generalized dressed spin susceptibility can be calculated from the Bethe-Salpeter equation as^{11,12}

$$\chi^m(Q) = [1 - \chi_{ph}^0(Q) \Gamma^{m,irr}(Q)]^{-1} \chi_{ph}^0(Q). \quad (2)$$

where bold quantities are matrices. The bubble susceptibility is defined as

$$[\chi_{ph}^0(Q)]_{K,K'} = -(N\beta)G(K+Q)G(K)\delta_{K,K'}. \quad (3)$$

Here, $G(K)$ is the dressed particle propagator, $K \equiv (\mathbf{k}, i\omega_m)$ denotes momentum/energy four-vectors (the lattice is two-dimensional), N is number of \mathbf{k} -points and $\beta = 1/(k_B T)$. In Eq. (2), $\Gamma^{m,irr}$ is the irreducible vertex function describing the irreducible interaction of the two elementary excitations. Eq. (2) is the common part of the response to an external field and solely depends on the electronic structure of the system. An observable response function, on the other hand, is obtained by closing the external legs of Eq. (2) using appropriate oscillator matrix elements, $O(Q)$ and $O(-Q)$, i.e.,

$$\chi_{obs}^m(Q) = \frac{1}{N^2 \beta^2} \sum_{KK'} O_{K,Q} [\chi^m(Q)]_{KK'} O_{K',-Q}. \quad (4)$$

The oscillator matrix elements depend on the orbital wave-function and the field wave-vector and frequency.¹³ In the $\mathbf{q} \rightarrow 0$ and $\nu_n \rightarrow 0$ limit, with an orthonormal basis set, the oscillator matrix element in the magnetic channel of a single-band system reduces to the identity multiplied by 1/2 due to the definition of spin in terms of electron densities, i.e., $S^z = (n_\uparrow - n_\downarrow)/2$.

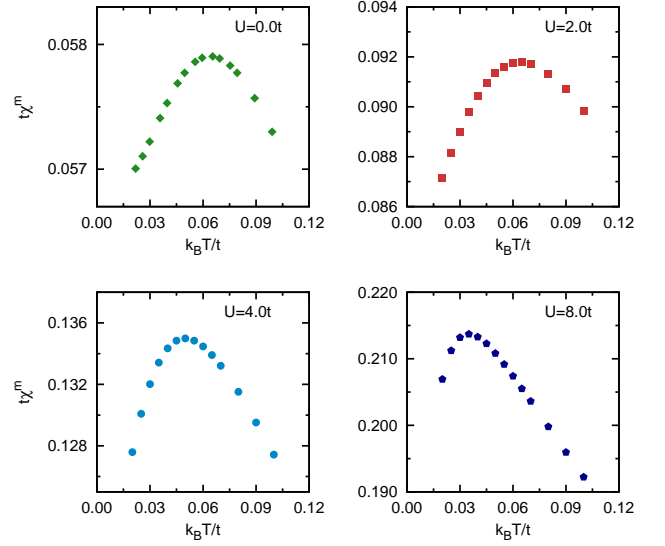


FIG. 2. Knight shift $K_S \propto \chi^m$ as a function of temperature $k_B T/t$ for $U = 0.0t$, $U = 2.0t$, $U = 4.0t$ and $U = 8.0t$. The electron density is $n = 0.9$. The peak position of the Knight shift moves to lower temperature upon increasing U .

We solve the Hamiltonian, Eq. (1), using DMFT and the exact diagonalization (ED) method¹⁴. In general, $[\Gamma^{m,irr}(Q)]_{K,K'}$ depends on the transferred momentum/frequency in a scattering process, Q , and on the incoming momentum/frequency variables. The out-coming variables are determined by conservation laws. In a normal system, there is a range and a characteristic relaxation time, beyond which $[\Gamma^{m,irr}(Q)]_{K,K'}$ becomes negligible. Hence, the spatially local part of the irreducible vertex function is the dominant part. This part of the irreducible vertex function, $[\Gamma_{loc}^{m,irr}(\nu_n)]_{\omega_m \omega_{m'}}$, can be calculated in the framework of the DMFT approximation from four point correlation functions on the self-consistent impurity¹⁵⁻¹⁷. A common approximation consists in substituting the irreducible vertex function by $\Gamma_{loc}^{m,irr}(\nu_n)$ and neglecting the non-local part¹⁸. The DMFT(ED) algorithm is also used to compute the local part of the irreducible vertex function^{15,16,18}.

Results – Figure 1 shows the Knight shift $K_S \propto \chi^m$ of the non-interacting system as a function of temperature for several electron densities. At $T \rightarrow 0$, the Knight shift saturates to $\rho(\epsilon_F)/4$. Upon increasing temperature, the thermal function $(dn(\epsilon)/d\epsilon)$ broadens, leading to a finite contribution of the vHS to the spin susceptibility. Hence, initially, the spin susceptibility upon increasing temperature, exhibits a broad maximum at T^* and then monotonically decrease beyond, following approximately a Curie-Weiss law for higher temperatures. The high- T reduction in the magnetic susceptibility is due to fast dynamics of electron spins. The maximum in the Knight shift becomes more pronounced and occurs at lower temperature for larger electron densities, namely, when the Fermi level, ϵ_F , approaches the vHS ϵ_{vHS} . At $n = 1$, where the Fermi energy lies on the vHS energy, the maximum oc-

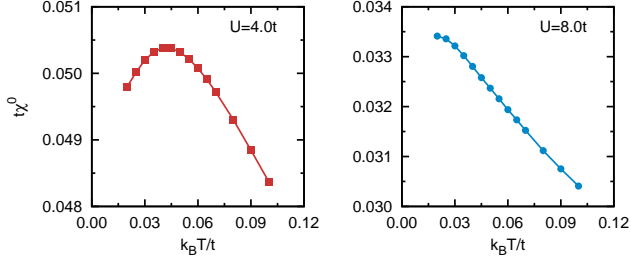


FIG. 3. Dressed bubble susceptibility as a function of temperature $k_B T/t$ for $U = 4.0t$ (left) and $U = 8.0t$ (right). The electron density is $n = 0.9$. At larger U values, the dressed bubble susceptibility does not show a downturn near the T^* calculated including vertex corrections.

curs at $T = 0$. Even in the non-interacting level, this trend is consistent with experimental results on AFe_2As_2 where T^* is the smallest for the Cs compound with the smallest energy difference $\epsilon_F - \epsilon_{vHS}$.

An interacting system is more polarizable than a non-interacting one. A Fermi-liquid system, for instance, exhibits an enhanced Pauli susceptibility given by $(1 + F_0^a)^{-1} \chi_0$ where $F_0^a < 0$ is Landau parameter. On the other hand, interactions broaden the vHS. Moreover, the response of an interacting system is not restricted to the electrons at the Fermi level but electrons around it also contribute. This raises the question of the impact of interactions on the above picture. Here, we restrict ourselves to weak to intermediate interaction strengths, which is appropriate for iron-based superconductors. The temperature dependence of K_S for $U = 2.0t$, $U = 4.0t$, and $U = 8.0t$ are shown in Fig. 2 and compared with the non-interacting case. As expected, the spin susceptibility is enhanced by interactions. Moreover, the downturn of χ^m at low T becomes more pronounced. The characteristic temperature, T^* , moves to lower temperatures upon increasing U . It is likely that the saturation of the spin susceptibility at very low T occurs at lower temperatures as interaction strength is increased. It is expected that AFe_2As_2 ($A = \text{K, Rb, Cs}$) compounds have similar interaction strengths, therefore the characteristic temperature is mainly determined by $\epsilon_F - \epsilon_{vHS}$.

Since evaluation of the irreducible vertex function is difficult, in real material calculations the spin susceptibility is often approximated with the dressed bubble diagram, Eq. (3). However, our calculations show that at large interaction strengths, the temperature dependence of the bubble susceptibility is different from the susceptibility calculated with vertex corrections. As can be seen from Fig. 3, in contrast to $U = 4.0t$ where the downturn of the spin susceptibility is present at the bubble level, for $U = 8.0t$ the bubble susceptibility increases upon decreasing T and does not show a downturn near the T^* calculated in Fig. 2, which includes vertex corrections. Therefore, it is essential to take into account vertex corrections for large values of the interaction to obtain the correct temperature dependence.

Furthermore, it is also customary to inspect the temper-

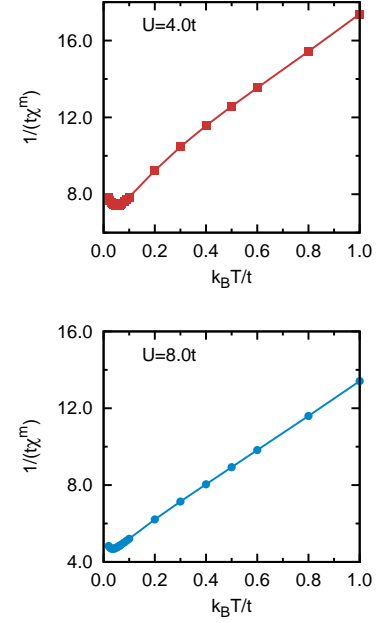


FIG. 4. Inverse spin susceptibility as a function of temperature $k_B T/t$ for $U = 4.0t$ (top) and $U = 8.0t$ (bottom). A Curie-Weiss law, $\chi_m^{-1}(T) \propto T + \theta$, becomes clearly established even at relatively low temperature (on electronic scales) for $U = 8.0t$. The electron density is $n = 0.9$.

ature dependence of the impurity susceptibility instead of $\chi^m(\mathbf{q} = \mathbf{0}, \nu_n = 0)$. Our results show that the downturn of $\chi^m(\mathbf{q} = \mathbf{0}, \nu_n = 0)$ cannot be seen from the impurity susceptibility. This can be understood if one assumes that, upon decreasing temperature, the dressed susceptibility at non-zero momenta grows faster than the reduction of $\chi^m(\mathbf{q} = \mathbf{0})$, hence, the local susceptibility, obtained from summation over all momenta, does not show the downturn seen in $\chi^m(\mathbf{q} = \mathbf{0})$.

Figure 4 displays the inverse spin susceptibility as a function of temperature. As can be seen from the figure, the temperature dependence of the spin susceptibility (Knight shift) at high temperature is consistent with a Curie-Weiss behavior, $\chi^m(T) \propto (T + \theta)^{-1}$. At very high temperature, of order of the bandwidth, the spin susceptibility approaches its value for localized non-interacting spins, i.e., $1/(4T)$ (not shown). A Curie-Weiss law, suggesting a local-moments dominated behavior, holds down to a lower temperature upon increasing interaction strength. As the temperature is decreased the susceptibility crosses-over from Curie-Weiss behavior to Fermi liquid behavior with a pronounced temperature dependence due to the proximity of the vHS.

The spin-lattice relaxation rate $1/(T_1 T)$ probes the low-frequency behavior of the spin susceptibility on the real axis. In a Fermi liquid state, a Korringa-like relaxation $1/(T_1 T) \sim \text{const.}$ is expected, whereas in a localized spin system $1/(T_1 T) \sim (T + \theta)^{-1}$. The experimental spin-lattice relaxation rates for AFe_2As_2 show a power-law dependence on temperature, $1/(T_1 T) \propto T^{-\eta}$. However, the exponent

changes around T^* : for $T < T^*$, $\eta \simeq 0.25$ while $\eta \simeq 1$ for $T > T^*$, although there are not enough data points for $T > T^*$ to be conclusive².

When the wave vector-dependence of the hyperfine interaction is neglected, the spin relaxation rate is given by¹⁹

$$\frac{1}{T_1 T} \propto \lim_{\nu \rightarrow 0} \left(\frac{1}{N} \right) \sum_{\mathbf{q}} \frac{\text{Im} \chi(\mathbf{q}, \nu)}{\nu}. \quad (5)$$

We use Padé analytic continuation for the impurity susceptibility at $U = 4.0t$, which is the best DMFT approximation for the local susceptibility. We find that $1/T_1 T$ is almost temperature-independent for $T < aT^*$ while it decreases upon increasing temperature for $T > aT^*$ (not shown), where a is a multiplicative factor slightly larger than unity. We believe $a \neq 1$ may be an artefact of the analytic continuation. Indeed, we can also analytically continue to zero-frequency using the approximation $(1/N) \sum_{\mathbf{q}} \chi(\mathbf{q}, \tau = 1/2T)/(\pi T^2)$, where τ denotes imaginary time²⁰. This is correct if $\text{Im} \chi(\mathbf{q}, \nu)/\nu$ remains frequency independent for $\nu < 2T$. This condition is not fully satisfied here. However, by employing this equation we find a change in $1/T_1 T$ temperature dependence behavior at T^* . Therefore, the relaxation rate temperature-dependence changes around the characteristic temperature in agreement with experimental results, however, η values do not fully agree. In our calculation, $1/T_1 T \sim 1/(T + \theta)$ for $T > T^*$.

Conclusion – Using the Hubbard model on the two-dimensional square lattice, we showed that a downturn in temperature-dependence of the spin susceptibility takes place with a characteristic temperature T^* . The characteristic temperature scales with the difference in energy between the Fermi level and the van Hove singularity. When vertex corrections are included with the DMFT-dressed propagators, the effect of the van Hove singularity seen in the non-interacting case is amplified and T^* moves to lower temperatures. Hence, given ARPES data on the proximity between the van Hove singularity and the Fermi level in AFe_2As_2 ($A = \text{K, Rb, Cs}$), this could naturally explain the main qualitative features of the measured Knight shift, without appeal to an orbital-selective Mott transition.

ACKNOWLEDGMENTS

We are deeply indebted to A.-M.S. Tremblay for insightful discussions and for careful reading of the manuscript. R. N is thankful to P. Richard for useful discussions. This work has been supported by the the Canada First Research Excellence Fund, the Natural Sciences and Engineering Research Council of Canada (NSERC) under grant RGPIN-2014-04584, and by the Research Chair in the Theory of Quantum Materials. Simulations were performed on computers provided by the Canadian Foundation for Innovation, the Ministère de l'Éducation des Loisirs et du Sport (Québec), Calcul Québec, and Compute Canada.

-
- ¹ K. R. Shirer, A. C. Shockley, A. P. Dioguardi, J. Crocker, C. H. Lin, N. apRoberts Warren, D. M. Nisson, P. Klavins, J. C. Cooley, Y.-f. Yang, and N. J. Curro, *Proceedings of the National Academy of Sciences* **109**, E3067 (2012), <http://www.pnas.org/content/109/45/E3067.full.pdf>.
 - ² Y. P. Wu, D. Zhao, A. F. Wang, N. Z. Wang, Z. J. Xiang, X. G. Luo, T. Wu, and X. H. Chen, *Phys. Rev. Lett.* **116**, 147001 (2016).
 - ³ F. Hardy, A. E. Böhm, D. Aoki, P. Burger, T. Wolf, P. Schweiss, R. Heid, P. Adelman, Y. X. Yao, G. Kotliar, J. Schmalian, and C. Meingast, *Phys. Rev. Lett.* **111**, 027002 (2013).
 - ⁴ D. Zhao, S. J. Li, N. Z. Wang, J. Li, D. W. Song, L. X. Zheng, L. P. Nie, X. G. Luo, T. Wu, and X. H. Chen, *Phys. Rev. B* **97**, 045118 (2018).
 - ⁵ L. de' Medici, G. Giovannetti, and M. Capone, *Phys. Rev. Lett.* **112**, 177001 (2014).
 - ⁶ K. Haule and G. Kotliar, *New Journal of Physics* **11**, 025021 (2009).
 - ⁷ A. Georges, L. d. Medici, and J. Mravlje, *Annual Review of Condensed Matter Physics* **4**, 137 (2013).
 - ⁸ Z. P. Yin, K. Haule, and G. Kotliar, *Nature Materials* **10**, 932 (2011).
 - ⁹ D. Fang, X. Shi, Z. Du, P. Richard, H. Yang, X. X. Wu, P. Zhang, T. Qian, X. Ding, Z. Wang, T. K. Kim, M. Hoesch, A. Wang, X. Chen, J. Hu, H. Ding, and H.-H. Wen, *Phys. Rev. B* **92**, 144513 (2015).
 - ¹⁰ P. Richard, A. van Roekeghem, X. Shi, P. Seth, T. K. Kim, X. H. Chen, S. Biermann, and H. Ding, (2018), [arXiv:1807.00193](https://arxiv.org/abs/1807.00193).
 - ¹¹ N. E. Bickers, "Self-consistent many-body theory for condensed matter systems," (Springer-Verlag, New York, 2004) Chap. 6, pp. 237–296.
 - ¹² R. Nourafkan, G. Kotliar, and A.-M. S. Tremblay, *Phys. Rev. Lett.* **117**, 137001 (2016).
 - ¹³ R. Nourafkan and A.-M. S. Tremblay, *Phys. Rev. B* **96**, 125140 (2017).
 - ¹⁴ M. Caffarel and W. Krauth, *Phys. Rev. Lett.* **72**, 1545 (1994).
 - ¹⁵ A. Toschi, A. A. Katanin, and K. Held, *Phys. Rev. B* **75**, 045118 (2007).
 - ¹⁶ G. Rohringer, A. Valli, and A. Toschi, *Phys. Rev. B* **86**, 125114 (2012).
 - ¹⁷ R. Nourafkan, M. Côté, and A. M. S. Tremblay, "Charge-fluctuations in lightly hole-doped cuprates: effect of vertex corrections," (2018), [arXiv:1807.03855](https://arxiv.org/abs/1807.03855).
 - ¹⁸ A. Georges, G. Kotliar, W. Krauth, and M. J. Rozenberg, *Rev. Mod. Phys.* **68**, 13 (1996).
 - ¹⁹ T. Moriya, *Progress of Theoretical Physics* **16**, 23 (1956).
 - ²⁰ M. Randeria, N. Trivedi, A. Moreo, and R. T. Scalettar, *Phys. Rev. Lett.* **69**, 2001 (1992).